



## Urban haze and photovoltaics†

I. M. Peters,<sup>a</sup> S. Karthik,<sup>b</sup> H. Liu,<sup>c</sup> T. Buonassisi<sup>a</sup> and A. Nobre<sup>b</sup>

Cite this: *Energy Environ. Sci.*, 2018, **11**, 3043

Received 13th April 2018,  
Accepted 3rd August 2018

DOI: 10.1039/c8ee01100a

rscl.li/ees

Urban haze is a multifaceted threat. Foremost a major health hazard, it also affects the passage of light through the lower atmosphere. In this paper, we present a study addressing the impact of haze on the performance of photovoltaic installations in cities. Using long-term, high resolution field data from Delhi and Singapore we derive an empirical relation between reduction in insolation and fine particulate matter (PM<sub>2.5</sub>) concentration. This approach enables a straightforward way to estimate air pollution related losses to photovoltaic power generation anywhere on the planet. For Delhi, we find that insolation received by silicon PV panels was reduced by  $11.5\% \pm 1.5\%$  or  $200 \text{ kWh m}^{-2}$  per year between 2016 and 2017 due to air pollution. We extended this analysis to 16 more cities around the planet and estimated insolation reductions ranging from 2.0% (Singapore) to 9.1% (Beijing). Using spectrum data from Singapore, we projected how other photovoltaic technologies would be affected and found an additional reduction compared to silicon of between 23% relative for GaAs and 42% for a 1.64 eV perovskite material. Considering current installation targets and local prices for electricity, we project that annual losses in revenue from photovoltaic installations could exceed 20 million USD for Delhi alone, indicating that annual economic damage from air pollution to photovoltaic site operators and investors worldwide could be billions of dollars.

### Broader context

Air pollution in cities is a serious issue and one that has grown more urgent in recent years. While the primary concern of urban air pollution is its impact on human health, there are additional detrimental effects to consider. In this paper we investigate how fine particulate matter in the air affects the energy yield of photovoltaic installations. Fine particulate matter is predominantly anthropogenic and is a main contributor to haze events. Correlating measured particulate concentrations and solar insolation in Delhi we find that 12.5% of the incoming light is extinct for every  $100 \mu\text{g m}^{-3}$  particle concentration. Using this relation we project that total sunlight reaching the ground in Delhi during one year is reduced by more than one ninth due to air pollution. This amount corresponds to  $40 \text{ kWh m}^{-2}$  yearly energy generated for a 20% efficient silicon solar panel. Even higher relative losses must be expected for solar cells with a band gap greater than that of silicon. Transferring our findings to several cities around the planet, we estimate that the economic damage due to losses in photovoltaic energy production caused by air pollution could be in the hundreds of millions of dollars annually.

## Motivation

In June 2013, three of the authors of this paper, I. M. Peters, L. Haohui and A. Nobre, lived in Singapore and were witnesses of the most severe haze event to have occurred in the city to date. For a couple of days, the pollutant standard index (PSI) jumped from its usual value of about 25 to over 200. The normally clear view from our office windows on the sixth floor became filled with an impenetrable fog that swallowed up neighboring buildings. Face masks were sold out in a matter of hours. People were panicking.

The event, in many ways, served as a wake-up call. Given our research focus on photovoltaic installations, we wanted to investigate the impact of haze on solar cell performance. From the reduced visibility it was evident that haze must have an effect, and we set out to quantify it. This paper summarizes our understanding so far. We have since learned about the devastating effects of urban air pollution on human health. This paper adds another aspect – the detrimental effect on photovoltaic power generation due to the reduction of light received. We hope that, in a small way, we can help raise awareness and make progress to improve the quality of life in what more and more people call home in the 21st century – cities.

## Introduction

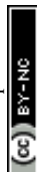
Air pollution in cities is a problem of growing urgency.<sup>1</sup> According to the World Health Organization (WHO), global urban air

<sup>a</sup> Massachusetts Institute of Technology, 77 Massachusetts Ave., 35-213, Cambridge, Massachusetts, USA. E-mail: [impeters@mit.edu](mailto:impeters@mit.edu)

<sup>b</sup> Cleantech Energy Corporation, O&M, 25 Church Street #03-04, Capital Square 3, Singapore, Singapore

<sup>c</sup> National University of Singapore Solar Energy Research Institute of Singapore, Singapore, Singapore

† Electronic supplementary information (ESI) available. See DOI: 10.1039/c8ee01100a



pollution levels have increased by 8% between 2008 and 2013.<sup>2</sup> The highest urban air pollution levels were observed in low- and middle-income cities in the Eastern Mediterranean and Southeast Asia. More than 80% of people living in monitored urban areas were exposed to air quality levels that exceed WHO limits.<sup>2</sup>

Air pollution typically includes ozone, small- (PM<sub>10</sub>) and fine (PM<sub>2.5</sub>) particulate matter.<sup>3</sup> Fine particulate matter describes particles with a diameter of less than 2.5  $\mu\text{m}$ . The primary sources of these particles are incomplete combustion, automobile emission, dust and cooking. In its majority, they are anthropogenic, with major composites being sulfates, nitrates, ammonia, carbon, lead and organic matter. Due to their small size, PM<sub>2.5</sub> particles are a major health hazard, because they can enter lungs and bloodstreams of humans. They give rise to chronic damage to the respiratory- and cardiovascular system<sup>4,5</sup> and contribute to premature mortality rates.<sup>6a,b</sup> WHO estimates that air pollution causes about 6.5 million premature deaths every year.<sup>7b</sup>

Apart from devastating effects on health, PM<sub>2.5</sub> particles are also the main cause of haze – periods with reduced visibility occurring in urban areas all around the world.<sup>7a-h</sup> Fig. 1 shows examples of how haze changes visibility in six cities. The change in visibility is related to a reduction in solar intensity and an alteration of the spectrum reaching the ground. In this study we focus on quantifying the impact of haze on insolation levels in cities, and the reduction in power generated by photovoltaic panels due to this effect. Until 2050, it is expected that 2.5 billion people will live in urban areas.<sup>8</sup> City integrated photovoltaics (PV) offer opportunities of mitigating challenges related to the high power demand of these growing urban areas.<sup>9,10</sup>

Surprising to the authors, it was difficult to assess the global capacity of PV installations in cities, based on literature data.

However, there are numerous indicators that a significant PV capacity is installed in urban areas, and more is to come. The potential for rooftop solar PV installations in cities was estimated at 5.4 TW – 70% of the electricity demand of urban residential and commercial consumers.<sup>10b</sup> Only a small fraction of this potential has been utilized so far. According to *Environment America*, in 2014, 6.5% of the solar PV capacity in the United States, or 1.3 GW, were installed in cities, with Los Angeles in the lead.<sup>11</sup> Several countries have formulated targets for rooftop installations, the most remarkable being India with 40 GW planned by 2022. China already has 22 GW of combined PV capacity installed on rooftops, and a further boost in rooftop installations is expected in 2018.<sup>12</sup> Australia had 16% of PV capacity installed on rooftops as of 2016. Furthermore, a growing number of cities have committed themselves to achieving 100% renewable electricity or energy. Examples include San Diego and San Francisco (California), Vancouver (Canada), Copenhagen (Denmark), Munich and Frankfurt (Germany). Other cities have formulated targets for renewable shares of total energy – e.g. Austin (Texas) 65% by 2025 and Paris (France) 25% by 2020 – or total electricity – e.g. Amsterdam (Netherlands), 50% by 2040, Canberra (Australia), 90% by 2020 and Tokyo (Japan) 24% by 2024.<sup>13</sup> While neither rooftop installations nor energy targets translate directly into PV installations in cities, they are indicators for the growing amount of solar panels installed in or near cities. There are also concrete targets for the installation of local renewable electric capacity in cities, including Los Angeles (1.3 GW of solar PV by 2020), New York (350 MW of PV by 2024) and San Francisco (950 MW renewables by 2020).<sup>13</sup>

The goal of this work is to correlate fine particulate matter concentration with a reduction of insolation reaching solar installations in cities. We start by analyzing pollution and



Fig. 1 Haze in Beijing.<sup>14</sup> Additional examples for Haze events around the world can be found in ref. 15–19.



insolation data collected in Delhi, India. The availability of high-quality, high-frequency insolation- and pollution data, as well as the high levels of pollution observed in Delhi make this city a suitable test case to observe the effects of air pollution. We apply a filtering method, introduced in ref. 7*h*, to find the functional relation between PM<sub>2.5</sub> concentration and relative reduction in insolation. We then use this functional relation to estimate haze related insolation losses in a number of cities around the globe, and to project the impact on different PV technologies. Finally, we attempt to estimate the economic damage resulting from air pollution related reductions in insolation.

## Correlating fine particle matter concentration and yield losses in Delhi

### I PM<sub>2.5</sub> concentration and insolation data

The collected data used in this analysis is summarized in Fig. 2. On the left hand side (a), measured insolation of a photovoltaic installation in Paschim Vihar, Delhi is shown. Insolation was recorded between May 2016 and November 2017 using two daily cleaned silicon sensors and a pyranometer with a frequency of one measurement every minute. The data shown in the figure was measured with one of the silicon sensors as this data is most representative of a silicon PV installation.

On the right hand side (b), PM<sub>2.5</sub> data recorded at the U.S. Embassy and Consulates' air quality monitors in Delhi<sup>20</sup> is depicted. The data is recorded with a frequency of one measurement per hour and made available through the "AirNow:" website of the Department of State.<sup>21</sup> The sensor is located in the Chanakyapuri area, approximately in 10 km air-line distance from the sensor measuring insolation. The distance between the two measurement stations adds an additional uncertainty to the correlation between them, as well as a number of unpredictable points. We discuss some of the consequences in the following.

Looking at the autocorrelation of the time series in Delhi, we find that PM<sub>2.5</sub> concentrations remain consistent for about 4 hours.

Considering the average wind speed of 10 km h<sup>-1</sup>,<sup>21</sup> we expect air pollution patterns to have an area on the order of tens of km<sup>2</sup> – an expectation that is supported by work done by Saraswat.<sup>22</sup> Lacking consistent, distributed measurements in Delhi, we additionally analyzed the correlation between PM<sub>2.5</sub> concentration measurements taken at five stations with similar distances in Singapore. The point to point correlation between the measured time series in those stations in 2017 was 0.6 ± 0.03. More relevant, however, is the correlation between the statistical distributions of pollution values. Comparing the five distributions using a LogNormal approximation, we find a relative variation of 5%. While these results cannot be directly transferred, they give an idea about the order of magnitude of how much the distance between measurement stations contributes to uncertainty. Note, however, that systematic temporal or spatial effects – for example predominant winds or local strong pollution sources are difficult to capture and constitute unpredictable factors.

To classify PM<sub>2.5</sub> concentration levels, we follow color coding for Air Quality Index (AQI) as suggested by AirNow.<sup>24</sup> Note, however, that AQI and PM<sub>2.5</sub> concentration are related but dissimilar metrics, hence pollution levels are not directly transferrable to AQI levels as typically used. Terminology and color coding is summarized in Table 1.

### II Correlating PM<sub>2.5</sub> concentration and loss in insolation

The methodology for relating PM<sub>2.5</sub> concentration to a reduction in insolation was introduced in ref. 7*h*. For a detailed description, we refer readers to this publication, though we provide a brief summary of the approach in the following. In ref. 7*h* we suggested sorting insolation data in bins corresponding to different levels of PM<sub>2.5</sub> concentration, and then use humidity and clear sky filters to identify data points representative of clear sky conditions.

We generally apply the same method here, yet with some alterations. The main difference between the analysis presented in ref. 7*h* and here is the length of time period considered.

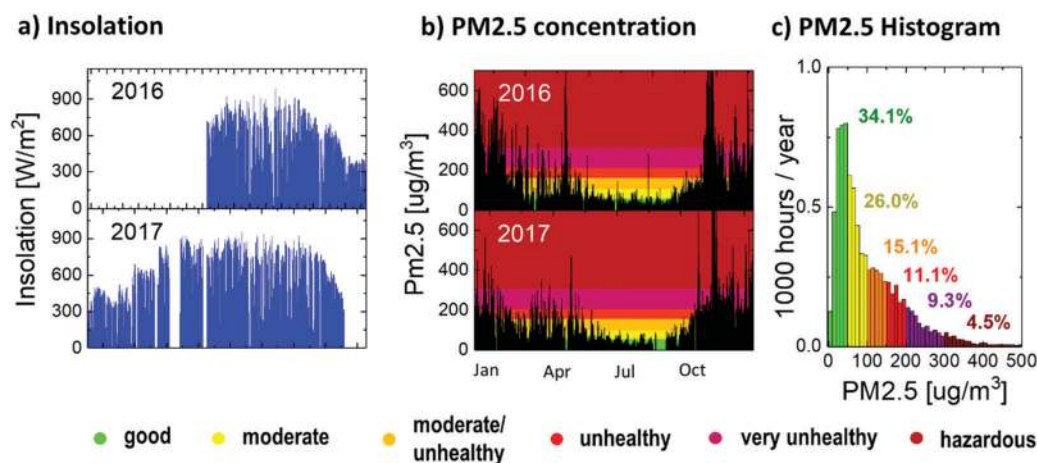


Fig. 2 (a) Delhi insolation measured with a silicon sensor between May 2016 and November 2017. (b) Delhi PM<sub>2.5</sub> concentration measured by the U.S. Embassy and Consulates' air quality monitors<sup>20,23</sup> (c) histogram of PM<sub>2.5</sub> concentration durations.



Table 1 PM2.5 concentration ranges and terminology

| Concentration range ( $\mu\text{g m}^{-3}$ ) | Color code | Levels of health concern |
|--|------------|--------------------------|
| 0–50   | Green      | Good                     |
| 51–100                                       | Yellow     | Moderate                 |
| 101–150                                      | Orange     | Moderately unhealthy     |
| 151–200                                      | Red        | Unhealthy                |
| 201–300                                      | Purple     | Very unhealthy           |
| Above 300                                    | Maroon     | Hazardous                |

In ref. 7h we analyzed a haze event that took place within 18 days. Here we consider insolation data over 19 months. Over the course of a year insolation varies *via* the zenith angle and the eccentricity of the Earth's orbit around the sun,<sup>25,26</sup> as well as due to seasonal variations in atmospheric conditions – *e.g.* water content. These variations need to be considered when analyzing correlations. For the purpose of this study, we considered

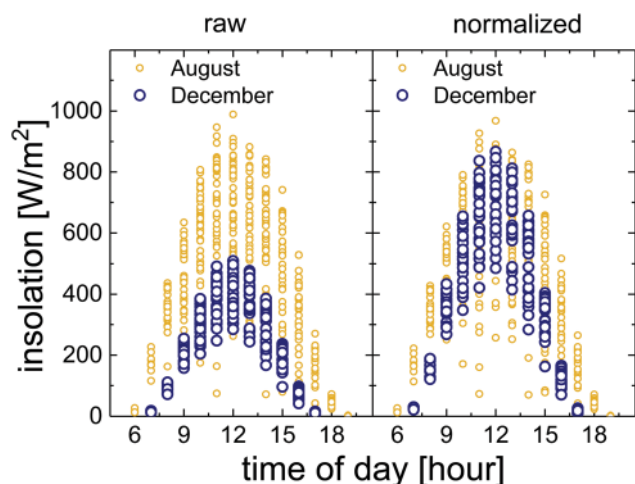


Fig. 3 Data measured in the months of August (yellow) and December (purple). On the left side the raw data is shown, on the right we show the data normalized to consider seasonal variations.

data for different months separately. Data of different months was later combined after normalizing it to the 90 percentile of all data points collected at noon for a given month. The effect of this normalization is shown in Fig. 3 for the examples of August and December, marking the months with highest and lowest overall insolation.

Fig. 4 illustrates how we correlate PM2.5 concentration levels with a reduction in insolation. Fig. 4a shows in steps how typical daily insolation curves for different pollution conditions are obtained. The figure on the left shows all available data points after adjustment for seasonal variations, with color coding indicating which pollution level they belong to. In the middle, two specific conditions are selected – moderate (50–100  $\mu\text{g m}^{-3}$ ) and very unhealthy (200–300  $\mu\text{g m}^{-3}$ ). The lines indicate the 80 percentile of the ensemble for each hour and pollution level. The 80 percentile filter here fulfills the same function as the combined humidity and clear sky filter in ref. 7h – *i.e.* it identifies conditions that are representative of a clear sky. The picture on the right, finally, shows the curves obtained for all six pollution levels. Note that only ensembles (*i.e.* data sets for a specific hour and pollution level) were considered that contained more than eight data points. This data was then used to generate Fig. 4b by considering the relative decrease in intensity as a function of PM2.5 concentration for each hour. Note that it is possible to correlation PM2.5 concentration and insolation reduction in a variety of different ways. We are discussing some of them in the ESI.<sup>1</sup> The important finding is that all ways we have tried resulted in similar functional correlations *i.e.* mono-exponential decays with exponents that were not significantly different.

Also shown in Fig. 4b are previous results from ref. 7h (cross shapes). These results are consistent with findings presented here. The advantage of the data set acquired in Delhi is the wide range of pollution conditions covered. Data ensembles with statistical relevance could be collected up to 375  $\mu\text{g m}^{-3}$  concentration, a factor three more than for Singapore. One consequence

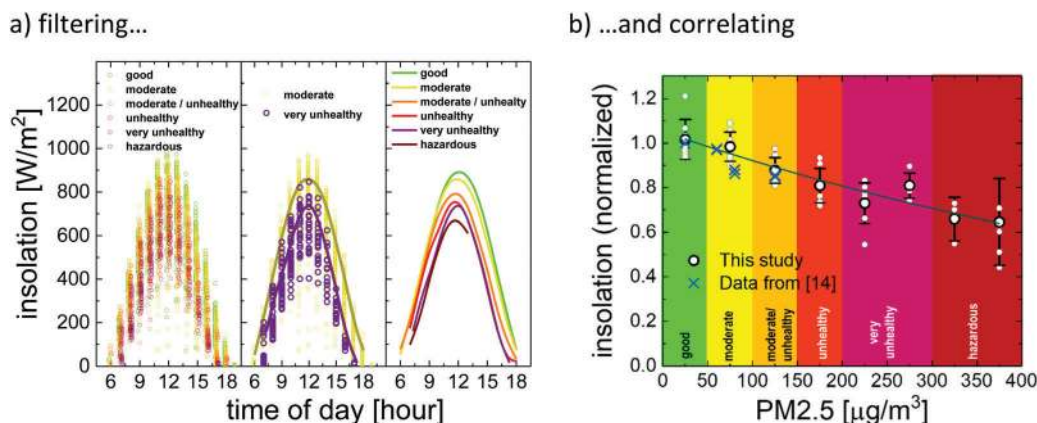


Fig. 4 (a) Sketch of how data points and typical curves for a clear day under specific pollution conditions are obtained. The figure on the left shows the data after adjustment for seasonal variations with a color code depending on pollution level. In the middle figure, two conditions are highlighted and curves are shown that represent the 80 percentile for the data ensemble of each hour. The figure on the right shows the curves obtained for all pollution conditions. In (b) this data is used to formulate a functional correlation between PM2.5 concentration and reduction of insolation by considering the relative reduction for each hour. Also shown are data obtained previously for Singapore<sup>7h</sup> and a mono-exponential decaying fit (see eqn (1)).





of this wider range is that the data presented here is slightly better represented by an exponential decay than by a linear function ( $R^2$  of 92% compared to 90%). Exponential decay is expected according to Lambert–Beer's law. The fitted exponential decay is shown as a blue line in the figure, and the functional relation is written down in eqn (1).

The function describing the exponential decay in Fig. 4b is summarized in the following equation. We will use this equation in the following to estimate how much light is lost due to air pollution. The uncertainty given here is calculated from least mean square fitting of a mono-exponential decay. Further details about this fit are given in the ESI.<sup>†</sup>

$$\frac{I(\text{PM2.5})}{I_0} = \exp\left(\frac{-\text{PM2.5}}{750 \pm 90}\right) \quad (1)$$

One caveat that needs to be mentioned concerns the composition of fine particulate matter. Composition changes over different time scales – within a day, seasonal,<sup>27</sup> and long-term.<sup>28</sup> We assume that the optical behavior of air pollution remains consistent within the investigated period and have tested this assumption by comparing results for specific months with the two year results shown in Fig. 4b, without finding significant differences. As shown in ref. 28, contributors to air pollution have significantly developed over the past 50 years, and it is possible that eqn (1) needs to be adjusted over long periods.

### III Haze related reduction in insolation and impact on a Si PV panel

The relation formulated in eqn (1) can directly be used to estimate the loss in yield due to a reduction in insolation due to haze. Fig. 5 summarizes the measured insolation for 2016 and 2017 from Fig. 2 in blue, and the estimated insolation at  $0 \mu\text{g m}^{-3}$  PM2.5 concentration in orange. The estimated curve was obtained by adjusting the measured insolation using the PM2.5 concentration measured at the same time. Integrating the insolation over the period of one year (May 2016 to May 2017), we obtain the annual radiant exposure as well as the projected exposure at  $0 \mu\text{g m}^{-3}$  PM2.5. These values are summarized in Table 2. The projected losses for Delhi are 11.5% of the annual solar energy or 200  $\text{kWh m}^{-2}$ . We have also included the projected yield losses for a 20% efficient silicon PV module.

**Projected losses in other cities.** Using the functional relation formulated in eqn (1), we extended the assessment of loss in

Table 2 PM2.5 impact on insolation in Delhi over one year

|   | Annual radiant exposure [ $\text{kWh m}^{-2}$ ] | Annual yield of a 20% Si-module [ $\text{kWh m}^{-2}$ ] |
|---|---|---|
| Measured data                           | 1570  | 314   |
| Projection $0 \mu\text{g m}^{-3}$ PM2.5 | $1770 \pm 30$                                   | $354 \pm 6$   |
| Ratio                                   | $88.5 \pm 1.5\%$                                |   |
| Difference                              | $200 \pm 30$                                    | $40 \pm 6$  |

annual radiant exposure to other cities. Several caveats have to be made at this point. The optical behavior of fine particulate matter depends on composition and size distribution. Both are known to vary substantially from location to location,<sup>29</sup> and it must be assumed that so do the optical characteristics.<sup>29</sup> Documents the compositional differences in great detail, including those for Singapore and Kanpur (India). The motivation for this projection is that, as shown in Fig. 4b, insolation losses for Singapore and Delhi are consistent despite the differences in composition. This consistency cannot be more than a first indicator and more detailed studies are required to establish how well eqn (1) can be transferred to other locations. In the following we make the assumption that eqn (1) is transferrable, but we ask the reader to keep in mind that the results should be interpreted in a qualitative way, rather than strictly quantitative. The cities covered in this study are shown in Fig. 6. We selected cities based on availability of air quality data, known haze events and geographic distribution.

Air quality data is available from a number of sources. For the results presented in this paper, we have used data from the AirNow Department of State (DOS) website.<sup>30</sup> This website provides historical data of PM2.5 measurements for a number of cities measured at U.S. embassies and consulates around the world. Depending on location, historical data dates back as far as 2015. For consistency reasons, we have made use of this database wherever possible. Additional sources we used (marked in blue) come from National or Communal centers and institutions.<sup>31–34</sup> The data obtained is summarized in Fig. 7.

Note that recordings for several cities are imperfect. Examples are Bogota in May and June 2017, Moscow in September 2017 and Richards Bay after October 2017. A dataset that does not cover a full year holds the threat of not correctly representing seasonal influences, which results in a hard to predict uncertainty. We have decided to still include the data for these cities, but ask the reader to consider this shortcoming when interpreting the results.

Using the data summarized in Fig. 7, and eqn (1), we can estimate the relative and absolute losses in radiant exposure. This estimate is summarized in Fig. 8 and Table 3. As we didn't have access to ground measured irradiance data for all locations, we used typical yearly irradiances, obtained from satellite data<sup>35</sup> and a clear sky model.<sup>28,36,37</sup> Satellite daily average irradiance data from NASA is available with a  $1 \times 1$  degree resolution. Irradiance for each day of the year over the course of ten years (2005–2015) was used, with the median value for each day marking the considered typical value (see ESI<sup>†</sup>). Daily irradiance distribution was projected with the clear sky model.

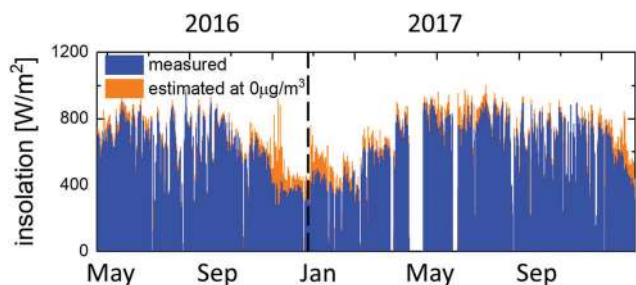


Fig. 5 Measured insolation (blue) and estimated insolation without air pollution, i.e. at a PM2.5 concentration of  $0 \mu\text{g m}^{-3}$  (orange).



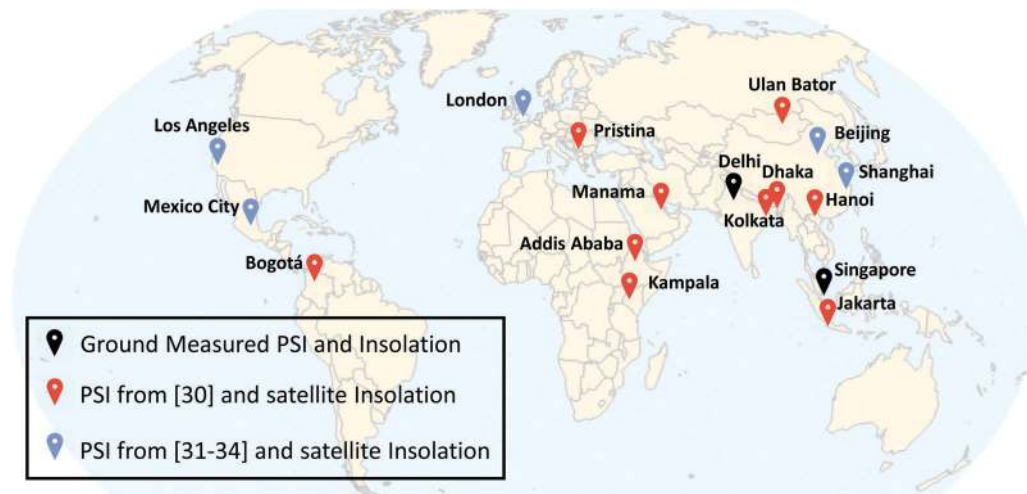


Fig. 6 Map of cities covered in this study. Black markers indicate locations for which simultaneous, ground-measured PM<sub>2.5</sub> and insolation data are available. Red markers indicate locations for which PM<sub>2.5</sub> data was obtained from ref. 30, for blue markers PM<sub>2.5</sub> data was taken from ref. 31–34.

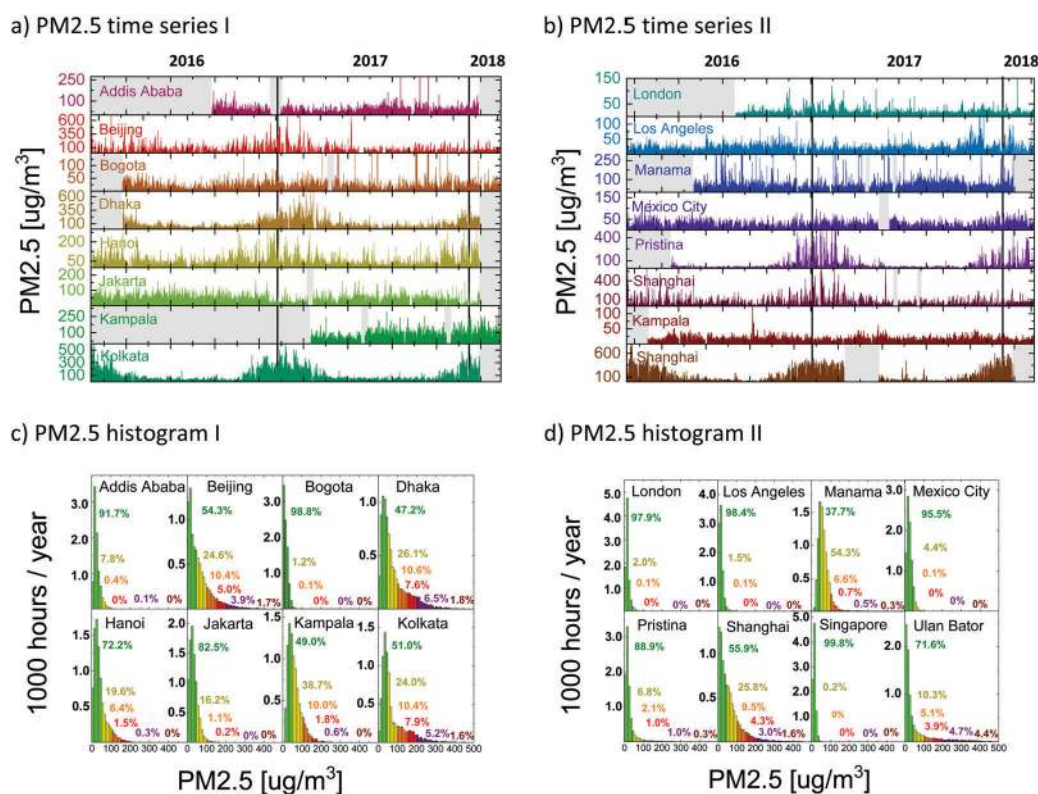


Fig. 7 Summary of PM<sub>2.5</sub> data obtained for cities shown in Fig. 6. (a) and (b) show the time series of the data obtained from ref. 30 and 31–34. Grey areas mark periods for which no data was available. (c) and (d) show the corresponding histograms of this data over the course of one year.

Corrections with eqn (1) were calculated on an hourly basis by reducing the incoming photon flux according to PM<sub>2.5</sub> concentration. This approach neglects contributions of clouds as well as ground reflection and scattering. Errors can be expected if such effects occur systematically at a specific time of day, as is the case, for example, in Singapore where morning tend to be sunnier than afternoons.<sup>38</sup> To benchmark this approach, we calculated the relative losses for Delhi (shown in the last column in Table 3a).

The calculated losses are  $12.2 \pm 0.9\%$ , which is consistent with the  $11.5 \pm 1.5\%$  obtained from ground based measurements.

To project the impact on photovoltaic panels, we have included two metrics in Table 3, the global tilted irradiation for fixed systems at optimum angle (GTI) in kWh m<sup>-2</sup>, and the photovoltaic power potential (PV<sub>out</sub>) in kWh per kWp. Values for these metrics for the different cities were obtained from the Global Solar Atlas.<sup>39</sup> Corrections and losses are calculated



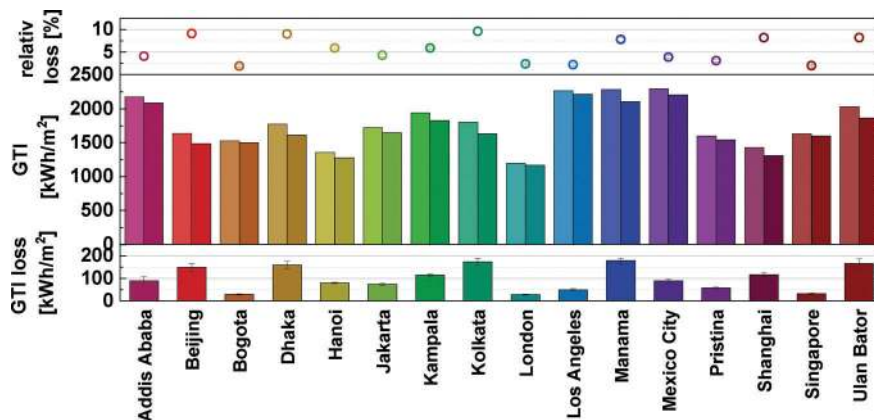


Fig. 8 Projected relative losses in radiant exposure for the considered cities – top, as well as tabulated global tilted irradiation for fixed systems at optimum angle (GTI) values according to ref. 37 (bright colors) and corrected values (dark) – middle. Absolute loss in GTI for each city is shown in the lower part of the figure.

**Table 3** (a) Projected relative losses in radiant exposure for the cities from Fig. 7(a) and (c), as well as tabulated and corrected GTI values, GTI losses and losses in PV power potential ( $PV_{out}$ ). (b) Projected relative losses in radiant exposure for the cities from Fig. 7(b) and (d), as well as tabulated and corrected GTI values, GTI losses and losses in PV power potential ( $PV_{out}$ ). Delhi is included as a reference to illustrate differences between ground based data and satellite based data

| (a)                           | Addis Ababa   | Beijing       | Bogota        | Dhaka         | Hanoi         | Jakarta       | Kampala       | Kolkata       |
|-------------------------------|---------------|---------------|---------------|---------------|---------------|---------------|---------------|---------------|
| Rel. loss [%]                 | $4.1 \pm 0.8$ | $9.1 \pm 1.0$ | $1.9 \pm 0.2$ | $9.0 \pm 0.9$ | $5.9 \pm 0.6$ | $4.3 \pm 0.4$ | $5.9 \pm 0.6$ | $9.6 \pm 1.0$ |
| GTI [ $kWh\ m^{-2}$ ]         | 2174          | 1634          | 1526          | 1774          | 1356          | 1721          | 1941          | 1804          |
| GTI corr. [ $kWh\ m^{-2}$ ]   | 2085          | 1485          | 1497          | 1614          | 1276          | 1647          | 1826          | 1631          |
| GTI loss [ $kWh\ m^{-2}$ ]    | $89 \pm 17$   | $149 \pm 16$  | $29 \pm 3$    | $160 \pm 16$  | $80 \pm 3$    | $74 \pm 5$    | $114 \pm 6$   | $173 \pm 14$  |
| $PV_{out}$ loss [kWh per kWp] | $71 \pm 14$   | $121 \pm 13$  | $24 \pm 2$    | $123 \pm 12$  | $62 \pm 2$    | $57 \pm 4$    | $89 \pm$      | $132 \pm 11$  |

| (b)                           | London        | Los Angeles   | Manama        | Mexico City   | Pristina      | Shanghai      | Singapore     | Ulan Bator    | Delhi          |
|-------------------------------|---------------|---------------|---------------|---------------|---------------|---------------|---------------|---------------|----------------|
| Rel. loss [%]                 | $2.4 \pm 0.2$ | $2.2 \pm 0.2$ | $7.8 \pm 0.8$ | $3.9 \pm 0.3$ | $3.6 \pm 0.4$ | $8.2 \pm 0.9$ | $2.0 \pm 0.2$ | $9.2 \pm 1.0$ | $12.2 \pm 1.2$ |
| GTI [ $kWh\ m^{-2}$ ]         | 1195          | 2267          | 2284          | 2295          | 1599          | 1428          | 1630          | 2031          | 1863           |
| GTI corr. [ $kWh\ m^{-2}$ ]   | 1166          | 2217          | 2106          | 2205          | 1541          | 1311          | 1597          | 1864          | 1636           |
| GTI loss [ $kWh\ m^{-2}$ ]    | $29 \pm 2$    | $50 \pm 5$    | $178 \pm 11$  | $90 \pm 7$    | $58 \pm 5$    | $117 \pm 10$  | $33 \pm 3$    | $167 \pm 20$  | $227 \pm 17$   |
| $PV_{out}$ loss [kWh per kWp] | $24 \pm 2$    | $39 \pm 4$    | $137 \pm 9$   | $71 \pm 5$    | $47 \pm 4$    | $94 \pm 8$    | $25 \pm 3$    | $144 \pm 18$  | $174 \pm 13$   |

directly by adjusting for the relative loss (first row). Uncertainties were obtained directly through the uncertainty in eqn (1) and indirectly by varying the beginning- and end point of the considered one year period.

**Projection to other PV technologies.** Losses in radiant exposure are not distributed uniformly across the solar spectrum. Data acquired in Singapore shows that shorter wavelengths are more affected, which is in line with expectations from basic scattering theory<sup>40</sup> and from studies showing stronger absorption at short wavelengths by nitrated and aromatic aerosol components in air pollution.<sup>41</sup> Hence, solar cells with a larger band gap should be more strongly affected than silicon. We projected the impact on other PV technologies by considering changes in absorption up to the band gap of the specific solar cell technology as a function of PM 2.5 concentration. Four band gaps were considered: silicon (1.12 eV) as baseline, GaAs (1.43 eV), CdTe (1.54 eV) and a material from the perovskite family (1.64 eV)<sup>42,43</sup> and four locations: Delhi, Beijing, Hanoi and Mexico City. The results of this exercise are shown in Fig. 9 and Table 4.

Compared to silicon, losses are projected to be increased by 23% for GaAs, 33% for CdTe and 42% for perovskites.

The presented analysis was performed for PV modules with an ideal tilt. Generally, we expect the results to also hold for one- or two axis tracked modules. Slight variations are likely, as PM2.5 concentrations show a systematic variation over the course of a day – in Delhi they are higher in the morning. In terms of absolute power generation, using data from ref. 44, a one-axis tracking system in Delhi would generate approx. 17% more energy, corresponding to a total loss in annual yield of  $47\ kWh\ m^{-2}$  for a 20% module (compare Table 2). For a two-axis tracking system, these numbers would change to approx. 19% or  $48\ kWh\ m^{-2}$ .

The situation is slightly different for bifacial modules. Bifacial modules use proportionally more diffuse light.<sup>45</sup> As haze increases the ratio of diffuse to direct light, bifacial modules will likely experience smaller losses than their mono-facial counterparts. A more elaborate optical measurement setup would allow exploring these aspects in more detail.





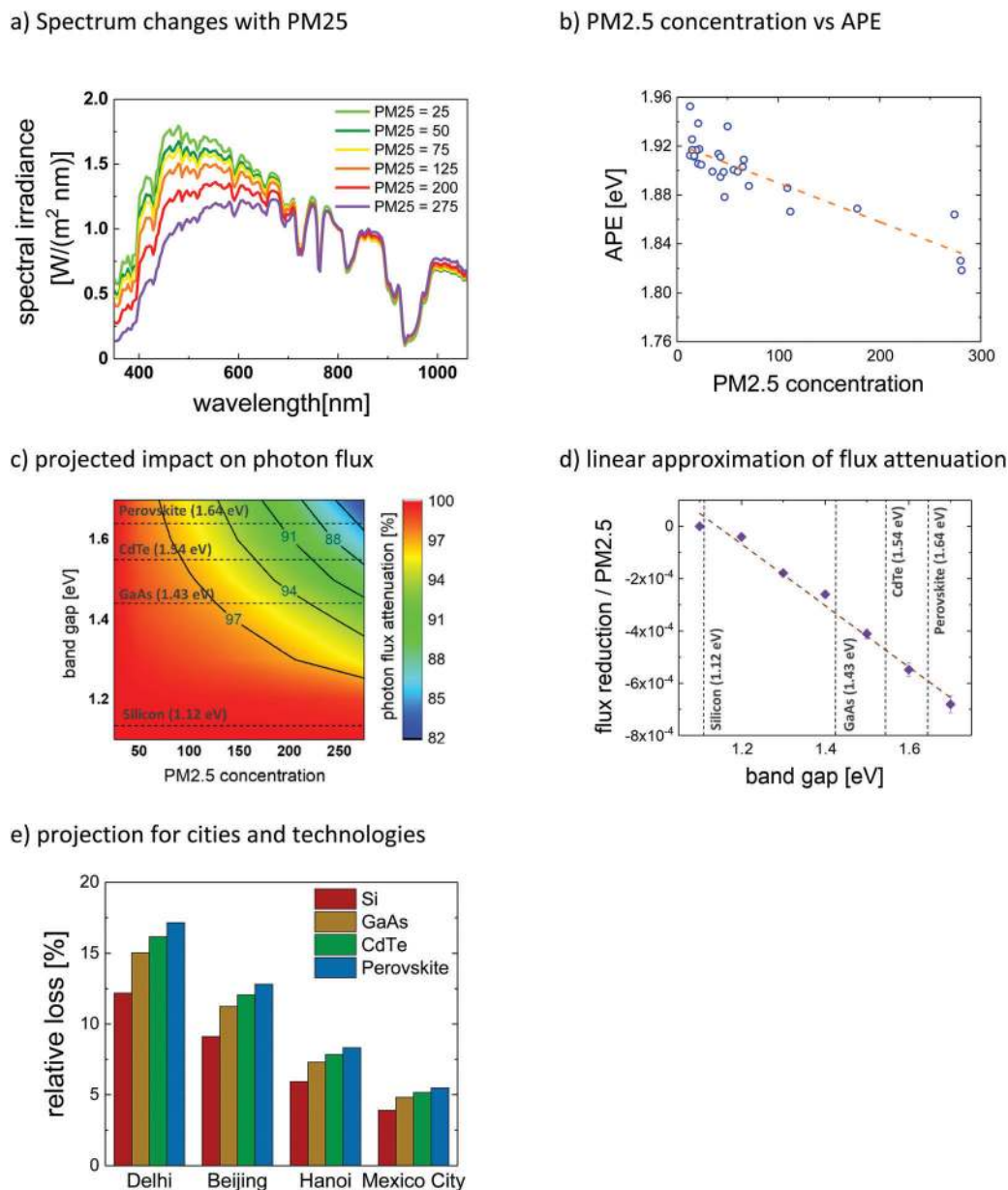


Fig. 9 Effect of fine particulate matter on different PV technologies. (a) Shows on examples how the solar spectrum is affected by different PM<sub>2.5</sub> concentrations. (b) Summarizes the relation between PM<sub>2.5</sub> concentration and average photon energy. The line is a guide to the eye. (c) Projects the impact of PM<sub>2.5</sub> concentration on the absorbed photon flux for absorbers with different band gaps. (d) Illustrates the reduction in photon flux per PM<sub>2.5</sub> concentration and band gap. In (e) this relation is used to project the PM<sub>2.5</sub> induced losses onto different PV technologies.

Table 4 Projected relative losses in absorbed photon flux for different PV technologies and four exemplary locations (compare Fig. 9e)

|             | Silicon<br>(1.12 eV) | GaAs<br>(1.43 eV) | CdTe<br>(1.54 eV) | Perovskite<br>(1.64 eV) |
|-------------|----------------------|-------------------|-------------------|-------------------------|
| Delhi       | 12.2                 | 15.0              | 16.1              | 17.2                    |
| Beijing     | 9.1                  | 11.2              | 12.0              | 12.8                    |
| Hanoi       | 5.9                  | 7.3               | 7.8               | 8.3                     |
| Mexico City | 3.9                  | 4.8               | 5.2               | 5.5                     |

**Economic considerations.** Using these numbers and Table 3, we can estimate the loss in revenue to PV installers and operators.

The average price for residential electricity in Delhi in January 2017 was 12.2 ct per kWh (8.07 rupees per kWh).<sup>46</sup> The estimated loss in PV power output is 174 kWh per kWp annually, resulting in a loss of 21.23 \$US per kWp each year – or 12% relative. Given the targets formulated by the Indian government, rooftop installations in Delhi can be expected to be in the GW range, which would put the annual damage to economy above 20 million dollars. Similarly, the estimated damage in Kolkata is 16 million dollars per GW.

In China, residential power prices are given as 7.9 ct per kWh (0.495 yuan per kWh) in Beijing and 9.1 ct per kWh (0.571 yuan per kWh) in Shanghai.<sup>47</sup> The estimated loss in





annual revenue here is 10 million dollars per GW installed for Beijing and 9 million dollars per GW installed in Shanghai.

However, even for cities with better air quality like Los Angeles air pollution causes notable economic damage. Average electricity costs for household electricity in Los Angeles in February 2018 were 18.4 ct per kWh<sup>48</sup> and 11.7 ct per kWh<sup>49</sup> for industry. Using the installation target of 1.3 GW by 2020, annual losses are between 5.9 and 9.3 million dollar.

## Discussion

### I Comparison to literature

Aerosols affect how sunlight passes through the atmosphere. This has been known since Tyndall observed that blue light is scattered more strongly than red light when passing through a clear fluid holding small particles.<sup>50</sup> And already Tyndall was concerned with the question how small particles that affect the passage of light would influence health. “Nor is the disgust abolished by the reflection that, although we do not see the nastiness, we are churning it in our lungs every hour and minute of our lives.” He writes in an article in *Nature* in 1870.<sup>51</sup> As discussed earlier, the concerns were well founded and numerous studies have confirmed the detrimental effects of haze on health – even if they are different than what Tyndall imagined.

Attempts to quantify the effect of aerosol particles on solar irradiance have also been made. A study by Husar *et al.*<sup>52</sup> and Guyemard *et al.*<sup>53</sup> looked at the effect on solar irradiation caused by two intense dust storms in the Gobi desert. When reaching the United States, the dust clouds resulted in a 30% reduction in direct normal solar radiation, and a 3.8% to 5.1% reduction in global horizontal irradiance (GHI). The increase in air pollution in China has triggered a number of studies that investigate the correlation between aerosols and solar irradiance. Li *et al.*<sup>54</sup> correlated satellite measured air pollution data and solar photovoltaic resource in China. They found that the combined aerosol optical depth of all particles reduced solar irradiance by 20–35%. Note that this study considers all aerosols in the atmospheric column, whereas results presented here only considers fine particulate matter.

We note that there is an increasing awareness of the role of air pollution on PV power generation, yet there are few studies quantifying the correlation between anthropogenic air pollution and a reduction in solar resource using ground-based measurements. One study looking into this was carried out by Jacobson.<sup>41</sup> In this paper UV absorption of nitrated aromatic aerosols and gasses in the boundary layer above Los Angeles (sea level to 1739 m altitude) was investigated. UV absorption of up to 50% was found, with global solar irradiance up until 2.8 μm wavelength reduced between 8 and 14%.

### II Air pollution and soiling

The work presented here only considers the reduction in solar resource due to light extinction caused by PM2.5 particles in the lower atmosphere. Air pollution causes an additional reduction in PV performance by dust accumulation on the solar panel. A discussion about the impact of different types of

aerosols is given in ref. 55, a general overview of the field is given in ref. 56.

### III Threats and opportunities

Solar Photovoltaics are both affected by air pollution and could provide a way to reduce it. One example: approximately 2.8 billion people cook with solid fuels, rendering cooking one of the prevalent sources of fine particulate matter in India, Pakistan and Southern Africa.<sup>57</sup> Solar or PV powered cookers<sup>58,59</sup> provide an almost pollution free alternative, and generally solar energy is thought to play an important role in improving air quality.<sup>60,61</sup> However, air pollution induced scattering and extinction of light reduces the available solar resource and increase the fraction of diffuse light. These effects, if not considered correctly, can make solar powered application underperform and become unreliable<sup>62,63</sup> – a threat to wide-spread adoption.

Policy makers in many regions are now acting to address air pollution issues. Dedicated Policies and the use of renewable energy sources can improve air quality, as many cities around the world have demonstrated. Notable examples include Vittoria-Gasteiz (Spain), Montréal (Canada), Lisbon (Portugal), Medellín (Colombia) and Seoul (South Korea), which managed to reduce air pollution between 28% and 63%.<sup>64</sup> China has drawn up an aggressive “battle plan” against smog that seems to have positive effects in cities like Beijing and Tianjin.<sup>65,66</sup> In a previous action plan (2013 to 2017), a 25% reduction in PM2.5 concentration was targeted. A reduction in PM2.5 concentration is visible in Fig. 7b for Beijing and Shanghai in the second half of 2017. Also India has formulated targets on reducing air pollution,<sup>67</sup> though recent news do not indicate significant improvements in air quality.<sup>68</sup>

## Summary and conclusions:

Urban haze is a threat with a multifaceted nature. It consists largely of anthropogenic fine particulate matter (PM2.5) generated to a large extent by incomplete combustion processes. Haze is a serious health hazard as it can penetrate deeply into the lungs and cause chronic damage to the respiratory system. Haze also affects the transition of light through the lower atmosphere, reducing the overall intensity of light reaching the ground and increasing the diffuse fraction.

### Relation between PM2.5 concentration and insolation

We analyze the relation between PM2.5 concentration and the loss in solar irradiance received by flat-panel silicon photovoltaic installations. Using long-term field data with high time-resolution from Delhi and Singapore, we introduce a functional relation that describes the measured data up until PM2.5 concentrations of 400 μg m<sup>-3</sup> and takes the form of a mono-exponential decay:

$$\frac{I(\text{PM2.5})}{I_0} = \exp\left(\frac{-\text{PM2.5}}{750 \pm 90}\right)$$

### Estimating insolation losses in Delhi

Using this function relation, we project how much insolation Delhi would have received if no air pollution was present for the



period between May 2016 and November 2017. We find that within a one-year period insolation was reduced by  $11.5 \pm 1.5\%$  or  $200 \text{ kWh m}^{-2}$  (from  $1770 \text{ kWh m}^{-2}$  to  $1570 \text{ kWh m}^{-2}$ ) by fine particulate matter.

### Projection to other cities

Using available air quality data and satellite measured insolation, we extended this analysis to 16 more cities in Africa (Addis Ababa, Kampala), the Americas (Bogota, Los Angeles, Mexico City), Asia (Beijing, Dhaka, Hanoi, Jakarta, Kolkata, Manama, Shanghai, Singapore, Ulan Bator) and Europe (London, Pristina). Repeating the analysis for Delhi, we found that using satellite data for a typical year (2006–2015) resulted in estimated losses that are consistent with those obtained from analyzing field measurements ( $12.2 \pm 0.9\%$ ). Estimated losses range from 2.0% relative or  $29 \text{ kWh m}^{-2}$  per year (Singapore) to 9.1% relative or  $149 \text{ kWh m}^{-2}$  per year (Beijing). We also projected losses in PV power potential and obtained values ranging from 24 kWh per kWp (London) to 144 kWh per kWp (Ulan Bator). Note that these results assume that average optical properties of air pollution in all locations are similar and should be taken with a grain of salt.

### Projection to other PV technologies

Using spectrum measurements from Singapore, we also projected how haze affects different PV technologies. Haze affects blue light stronger than red light, resulting in PV materials with larger band gaps being more affected than silicon. Adjusting for additional current losses we predict that losses increase by 23% relative for GaAs, 33% for CdTe and 42% for perovskites (at 1.64 eV band gap) compared to silicon.

### Economic implications

Reduced insolation results in lost revenues for system operators and investors in PV systems. Given the aggressive installation goals for many countries and communities, installations in urban areas in the order of GW can be expected. For installations of this magnitude and current electricity prices, projected annual losses in revenue for Delhi could well exceed 20 million dollars, or 12% of total revenue. Similarly, projected losses for GW installations would suffer annual losses of 16 million dollars in Kolkata and around 10 million dollars in Beijing and Shanghai. In Los Angeles with a target capacity of 1.3 GW of installed solar by 2020, projected annual economic losses are between 6 and 9 million dollars. These numbers indicate that global losses in revenue could easily amount to hundreds of millions, if not billions of dollars annually. An additional factor is that the reduced insolation and changed character of sunlight (more diffuse light), if not accounted for correctly, will affect the reliability of PV powered systems with a hard to quantify reduction in adoption.

### Conflicts of interest

There are no conflicts to declare.

## Acknowledgements

The authors thank Liu Zhe for help with Chinese websites and texts. This work was financially supported by funding from Singapore's National Research Foundation through the Singapore MIT Alliance for Research and Technology's "Low energy electronic systems (SMART-LEES) IRG" and by the DOE-NSF ERF for Quantum Energy and Sustainable Solar Technologies (QESST).

## References

- 1 J. Vidal, Air pollution rising at an 'alarming rate' in world's cities, *The Guardian*, 11 May 2016, <https://www.theguardian.com/environment/2016/may/12/air-pollution-rising-at-an-alarming-rate-in-worlds-cities>.
- 2 World Health Organization, Ambient air pollution: a global assessment of exposure and burden of disease, World Health Organization, 2016, pp. 1–131.
- 3 Hannah Ritchie and Max Roser – Air Pollution, 2017, Published online at OurWorldInData.org, Retrieved from: <https://ourworldindata.org/air-pollution>, [Online Resource].
- 4 K. Kornei, Here are some of the world's worst cities for air quality, *Science*, 2017, DOI: 10.1126/science.aal0942, <http://www.sciencemag.org/news/2017/03/here-are-some-world-s-worst-cities-air-quality>.
- 5 EPA, Overview of Particle Air Pollution, Presented at the Air Quality Communication Workshop, San Salvador, 2012.
- 6 The impact of pollution on health and mortality is well documented. These are just two prominent among many good examples: (a) J. Lelieveld, J. S. Evans, M. Fnais, D. Giannadaki and A. Pozzer, The contribution of outdoor air pollution sources to premature mortality on a global scale, *Nature*, 2015, **525**, 367–371; (b) R. Beelen, *et al.*, Effects of long-term exposure to air pollution on natural-cause mortality: an analysis of 22 European cohorts within the multicentre ESCAPE project, *Lancet*, 2014, **383**, 785–795.
- 7 There is a range of literature on haze in different locations, especially China. Examples are: (a) D. Mishra, P. Goyal and A. Upadhyay, Artificial intelligence based approach to forecast PM2.5 during haze episodes: a case study of Delhi, India, *Atmos. Environ.*, 2015, **102**, 239–248; (b) <http://www.who.int/airpollution/en/>; (c) R. Gottlieb and S. Ng, *Global Cities, Urban Environments in Los Angeles, Hong Kong, and China*, MIT Press, 2017; (d) M. Iftikhar, K. Alam, A. Sorooshian, W. A. Syed, S. Bibi and H. Bibi, Contrasting aerosol optical and radiative properties between dust and urban haze episodes in megacities of Pakistan, *Atmos. Environ.*, 2018, **173**, 157–172; (e) R. Zhang, *et al.*, Overview of Persistent Haze Events in China, in *Air Pollution in Eastern Asia: An Integrated Perspective*, ed. I. Bouarar, X. Wang and G. Basseur, ISSI Scientific Report Series, Springer, Cham, 2017, vol. 16; (f) G. Wang, *et al.*, Persistent sulfate formation from London Fog to Chinese haze, *PNAS*, 2016, **113**, 13630–13635; (g) H. Liu, *et al.*, The Impact of Haze on Performance Ratio and Short-Circuit Current of PV Systems in Singapore, *IEEE J. Photovolt.*, 2014, **4**, 1585–1592;



- (h) A. Nobre, *et al.*, On the impact of haze on the yield of photovoltaic systems in Singapore, *Renewable Energy*, 2016, **89**, 389–400.
- 8 United Nations Department of Economic and Social Affairs, Population Division, World Urbanization Prospects: The 2014 Revision, CD-ROM Edition, United Nations, 2014.
  - 9 D. M. Kammen and D. A. Sunter, City-integrated renewable energy for urban sustainability, *Science*, 2016, **352**, 922–927.
  - 10 (a) S. Castellanos, D. A. Sunter and D. M. Kammen, Rooftop solar photovoltaic potential in cities: how scalable are assessment approaches?, *Environ. Res. Lett.*, 2017, **12**, 125005; (b) IEA, Energy Technology Perspective 2016, Annex H – Rooftop Solar PV Potential in Cities, <https://www.iea.org/etp/etp2016/annexes/>.
  - 11 J. Burr, L. Hallock and R. Sargent, Shining Cities – Harnessing the Benefits of Solar Energy in America, EA Report 2015.
  - 12 PVMagazine, Rooftop PV key driver of 2017 installation forecast hike in China, Novemer 23rd 2017, <https://www.pv-magazine.com/2017/11/23/driving-forces-behind-chinas-2017-solar-boom/>.
  - 13 REN21, Renewables 2016, Global Status Report, Renewable Energy Policy Network, 2016, [http://www.ren21.net/wp-content/uploads/2016/06/GSR\\_2016\\_Full\\_Report.pdf](http://www.ren21.net/wp-content/uploads/2016/06/GSR_2016_Full_Report.pdf).
  - 14 <http://www.climatechangenews.com/2017/03/23/melting-arctic-worsens-beijings-pollution-haze-study-finds/>. Image reproduced with permission from J. Aaron Farr.
  - 15 <https://www.ecowatch.com/top-weather-events-2016-2180215649.html>.
  - 16 <http://www.bbc.com/news/uk-32233922>.
  - 17 <https://www.nbcnews.com/science/environment/cough-cough-climate-change-may-worsen-air-pollution-n136986>.
  - 18 <https://modern.diplomacy.eu/2017/12/21/cairos-bad-breath/>.
  - 19 <https://sds-was.aemet.es/events/4th-colombian-meeting-and-international-conference-on-air-quality-and-public-health>.
  - 20 Information about the Air Quality data measured by the U.S. Embassy and Consulates in India is provided here: <https://in.usembassy.gov/embassy-consulates/new-delhi/air-quality-data/>.
  - 21 <https://weatherspark.com/y/109174/Average-Weather-in-New-Delhi-India-Year-Round>.
  - 22 A. Saraswat, *Air Pollution in New Delhi, India: Spatial and Temporal Patterns of Ambient Concentrations and Human Exposure*, PhD thesis, University of British Columbia, 2015.
  - 23 Datasets for Delhi can be downloaded here: [https://www.airnow.gov/index.cfm?action=airnow.global\\_summary#India\\$New\\_Delhi](https://www.airnow.gov/index.cfm?action=airnow.global_summary#India$New_Delhi).
  - 24 <https://airnow.gov/index.cfm?action=aqibasics.aqi>.
  - 25 R. G. Allen, *Environmental, and E. Water Resources Institute. Task Committee on Standardization of Reference, The ASCE standardized reference evapotranspiration equation*, American Society of Civil Engineering, Reston, Va., 2005.
  - 26 M. J. Reno, C. W. Hansen and J. S. Stein, Global Horizontal Irradiance Clear Sky Models: Implementation and Analysis, Sandia Report, SAND2012-2398, Sandia National Laboratories, 2012.
  - 27 J. L. Hand, B. A. Schichtel, M. Pitchford, W. C. Malm and N. H. Frank, Seasonal composition of remote and urban fine particulate matter in the United States, *J. Geophys. Res.*, 2011, **117**, D05209.
  - 28 E. W. Butt, S. T. Turnock, R. Rigby, C. L. Reddington, M. Yoshioka, J. S. Johnson, L. A. Regayre, K. J. Pringle, G. W. Mann and D. V. Spracklen, Global and regional trends in particulate air pollution and attributable health burden over the past 50 years, *Environ. Res. Lett.*, 2017, **12**, 104017.
  - 29 G. Snider, *et al.*, Variation in global chemical composition of PM<sub>2.5</sub>: emerging results from SPARTAN, *Atmos. Chem. Phys.*, 2016, **16**, 9629–9653.
  - 30 The data for a number of cities is provided here: [https://airnow.gov/index.cfm?action=airnow.global\\_summary](https://airnow.gov/index.cfm?action=airnow.global_summary), (compare ref. 29).
  - 31 Data for Beijing and Shanghai was obtained from the China National Environmental Monitoring Centre (CNEMC), <http://www.cnemc.cn/>.
  - 32 Data for London was obtained from the London Air Quality Network (LAQN), <http://www.londonair.org.uk/LondonAir/General/about.aspx>.
  - 33 Data for Mexico City was obtained from Red Automática de Monitoreo Atmosférico (RAMA) of the city of Mexico, <http://www.aire.df.gob.mx/default.php?opc=%27aKBh%27>.
  - 34 Data for Los Angeles was obtained from the California Air Resource Board, <https://ww2.arb.ca.gov/>.
  - 35 Irradiance data is obtained from NASA's Clouds and the Earth's Radiant Energy System (CERES) website, <https://ceres.larc.nasa.gov/>.
  - 36 V. Badescu, Verification of some very simple clear and cloudy sky models to evaluate global solar irradiance, *Sol. Energy*, 1997, **61**, 251–264.
  - 37 R. G. Allen, *Environmental, and E. Water Resources Institute. Task Committee on Standardization of Reference, The ASCE standardized reference evapotranspiration equation*, American Society of Civil Engineers, Reston, Va., 2005.
  - 38 Y. S. Khoo, A. Nobre, R. Malhotra, D. Yang, R. Rüther, T. Reindl and A. Aberle, Optimal Orientation and Tilt Angle for Maximizing in-Plane Solar Irradiation for PV Applications in Singapore, *IEEE J. Photovolt.*, 2014, **4**, 647–653.
  - 39 <http://globalsolaratlas.info/>.
  - 40 J. Strutt, On the transmission of light through an atmosphere containing small particles in suspension, and on the origin of the blue of the sky, *Philos. Mag.*, 1899, **5**, 375–394.
  - 41 M. Z. Jacobson, Isolating nitrated and aromatic aerosols and nitrated aromatic gases as sources of ultraviolet light absorption, *J. Geophys. Res.*, 1999, **104**, 3527–3542.
  - 42 I. M. Peters, L. Haohui, T. Reindl and T. Buonassisi, Global Prediction of Photovoltaic Field Performance Differences Using Open-Source Satellite Data, *Joule*, 2018, **2**, 307–322.
  - 43 I. M. Peters and T. Buonassisi, Energy Yield Limits for Single Junction Solar Cells, *Joule*, 2018, **2**, 1160–1170.
  - 44 M. Z. Jacobson and V. Jadhav, World estimates of PV optimal tilt angles and ratios of sunlight incident upon tilted and tracked PV panels relative to horizontal panels, *Sol. Energy*, 2018, **169**, 55–66.





- 45 S. Guo, T. M. Walsh and I. M. Peters, Vertically mounted bifacial photovoltaic modules: A global analysis, *Energy*, 2013, **61**, 447–454.
- 46 R. Toniga, Delhi's Household Electricity Subsidies: Highly Generous but Inefficient? Brookings India IMPACT Series No. 042017, April 2017.
- 47 N. Zhou, Lawrence Berkeley National Laboratory China Energy Group, Key China Energy Statistics 2016, 2017, <https://china.lbl.gov/sites/default/files/misc/ced-9-2017-final.pdf>.
- 48 United States Department of Labor, Bureau of Labor Statistics, Average Energy Prices, Los Angeles-Long Beach-Anaheim – February 2018, [https://www.bls.gov/regions/west/news-release/averageenergyprices\\_losangeles.htm](https://www.bls.gov/regions/west/news-release/averageenergyprices_losangeles.htm).
- 49 <https://www.electricitylocal.com/states/california/los-angeles/>.
- 50 J. Tyndall, On Radiation through the Earth's Atmosphere, Proceedings of the Royal Institution, 1863.
- 51 J. Tyndall, On haze and dust, *Nature*, 1870, 339–342.
- 52 R. B. Husa, *et al.*, Asian dust events of April 1998, *J. Geophys. Res.*, 2001, **106**, 18317–18330.
- 53 C. A. Gueymard, C. N. S. Laulainen, J. K. Vaughan and F. E. Vignola, China's dust affects solar resource in the U.S.: a case study, SOLAR 2000, paper presented at the ASES Annual Conference, U.S. Dep. of Energy, Madison, Wisc., June 16–21, 2000.
- 54 X. Li, F. Wagner, W. Peng, J. Wang. and D. Mauzerall, Reduction of solar photovoltaic resources due to air pollution in China, *PNAS*, 2017, **114**, 11867–11872.
- 55 L. Micheli, M. Muller and S. Kurtz, Determining the effects of environment and atmospheric parameters on PV field performance, Proceedings of the 43rd IEEE PVSC, Portland OR, 2016.
- 56 S. C. S. Costa, A. S. A. C. Diniz and L. L. Kazmerski, Solar energy dust and soiling R&D progress: literature review update for 2016, *Renewable Sustainable Energy Rev.*, 2018, **82**, 2504–2536.
- 57 Z. A. Chafe, M. Brauer, Z. Klimont, R. Van Dingenen, S. Mehta, S. Rao, K. Riahi, F. Dentener and K. R. Smith, Household Cooking with Solid Fuels Contributes to Ambient PM<sub>2.5</sub> Air Pollution and the Burden of Disease, *Environ. Health Perspect.*, 2014, **122**, 1314–1320.
- 58 S. D. Pohekar and M. Ramachandran, Multi-criteria evaluation of cooking energy alternatives for promoting parabolic solar cooker in India, *Renewable Energy*, 2004, **9**, 1449–1460.
- 59 S. B. Joshi and A. R. Jani, Design, development and testing of a small scale hybrid solar cooker, *Sol. Energy*, 2015, **122**, 148–155.
- 60 Z. Peidong, Y. Yanli, S. Jin, Z. Yonghong, W. Lisheng and L. Xinrong, Opportunities and challenges for renewable energy policy in China, *Renewable Sustainable Energy Rev.*, 2009, **13**, 439–449.
- 61 M. Z. Jacobson, Review of solutions to global warming, air pollution, and energy security, *Energy Environ. Sci.*, 2009, **2**, 148–173.
- 62 S. Watson, D. Bian, N. Sahraei, A. G. Winter, T. Buonassisi and I. M. Peters, Advantages of operation flexibility and load sizing for PV-powered system design, *Sol. Energy*, 2018, **162**, 132–139.
- 63 N. Sahraei, S. M. Watson, A. Pennes, I. M. Peters and T. Buonassisi, Design approach for solar cell and battery of a persistent solar powered GPS tracker, *Jpn. J. Appl. Phys.*, 2017, **56**, 08ME01.
- 64 <http://talkofthecities.iclei.org/how-these-five-global-cities-have-improved-their-air-quality/>.
- 65 <https://www.reuters.com/article/us-china-pollution/china-puts-finishing-touches-to-three-year-smog-crackdown-plan-idUSKBN1FK095>.
- 66 <https://phys.org/news/2018-01-china-air-quality.html>.
- 67 <http://www.who.int/bulletin/volumes/94/7/16-020716/en/>.
- 68 <https://www.nytimes.com/2017/12/08/world/asia/india-pollution-modi.html>.

